

# Quantum geometry in correlated electron phases: from flat band to dispersive band

Taisei Kitamura,<sup>1,2</sup> Akito Daido,<sup>3</sup> and Youichi Yanase<sup>3</sup>

<sup>1</sup>*Department of Physics, Graduate School of Science, University of Tokyo, Tokyo 113-0033, Japan*

<sup>2</sup>*RIKEN Center for Emergent Matter Science (CEMS), Wako 351-0198, Japan*

<sup>3</sup>*Department of Physics, Graduate School of Science, Kyoto University, Kyoto 606-8502, Japan*

(\*[taisei-kitamura@g.ecc.u-tokyo.ac.jp](mailto:taisei-kitamura@g.ecc.u-tokyo.ac.jp))

(Dated: 3 March 2026)

Quantum geometry, describing the geometric properties of the Bloch wave function in momentum space, has recently been recognized as a fundamental concept in condensed matter physics. The flat-band system offers the paradigmatic platform where quantum geometry plays the essential role in correlated electron phases. However, systems that suffer from significant effects of quantum geometry are not limited to flat-band systems; dispersive-band systems also exhibit quantum condensed phases driven by quantum geometry. In this perspective, we provide a transparent account of quantum geometry and its role in correlated electron phases, throughout flat-band and dispersive-band systems.

## I. INTRODUCTION

The Hubbard model, which describes Bloch electrons experiencing many-body electron-electron interactions, is a minimal framework for studying correlated electron phases in solids. In its simplest form, the Bloch electrons are modeled by a single band, while the many-body interaction is represented by an on-site Coulomb repulsion. The single band Hubbard model has been suggested as a useful tool for describing various phenomena in condensed matter physics such as superconductivity and magnetism<sup>1,2</sup>. By contrast, correlated electron systems with nontrivial band structures have been intensively studied in modern condensed matter physics. Once the assumption of a "single-band model" is removed, Bloch electrons acquire nontrivial properties originating from their wave functions, and the topology of quantum matter becomes manifest<sup>3,4</sup>. Stimulated by the discovery of topological quantum phases, the importance of the Bloch wave function among a variety of phenomena in solid state systems has been recognized. For example, in research of transport phenomena, the geometric structure of the Bloch wave function in momentum space including the Berry curvature and the shift vector has been investigated since the 1980's<sup>5-7</sup>. This may be regarded as an early stage research of what we refer to here as "quantum geometry."

Early studies of quantum geometry primarily focused on phenomena in which many-body interactions play a subdominant role, and a variety of transport responses triggered by quantum geometry has been identified<sup>8,9</sup>. However, the physics of correlated electron systems driven by many-body interactions can also be influenced by the nontrivial properties of the Bloch wave function. For instance, in iron-based superconductors, antiferromagnetic fluctuations arising from nesting between disconnected Fermi surfaces require strong hybridization among the  $d$  electrons. This can be understood as a kind of quantum-geometric effects, since a nontrivial feature of the Bloch wave function is indispensable<sup>10</sup>. Moreover, in flat-band ferromagnetism, it is known that the overlap of

Wannier functions is crucial for the uniqueness of the ground state<sup>11</sup>; since the Fourier transform of a Wannier function is the Bloch wave function, this provides another example in which the nontriviality of the Bloch wave function plays an essential role.

These specific examples illustrate the necessity of a theoretical framework that enables a unified understanding of correlated electron phases emerging from the nontrivial geometric properties of the Bloch wave function in momentum space. This issue is solved by *quantum geometry*<sup>12,13</sup>. In fact, the two examples above can be understood within this framework<sup>14,15</sup>. Such a unified description utilizing the concept of quantum geometry not only allows for a deeper understanding of the established phenomena but also predicts the correlated electron phases driven by the nontrivial Bloch wave functions. Indeed, on the one hand, it has recently been recognized that flat-band systems offer a paradigmatic platform for studies of quantum geometry in correlated electron phases<sup>16-20</sup>. On the other hand, correlated electron phases in dispersive-band systems are also a growing research area of quantum geometry.

In this perspective, we propose a transparent picture of how Bloch electrons manifest quantum geometry and how quantum geometry underlies correlated electron phases, which encompasses systems ranging from flat bands to dispersive bands. We begin by reviewing quantum geometry in the context of correlated electron phases, focusing on flat-band systems. We then demonstrate that correlated electron phases in flat-band systems have counterparts in dispersive-band systems with nontrivial quantum geometry. In this way, we clarify the role of nontrivial quantum geometry in correlated phases of both flat-band and dispersive-band electron systems and elucidate the connection between these two regimes.

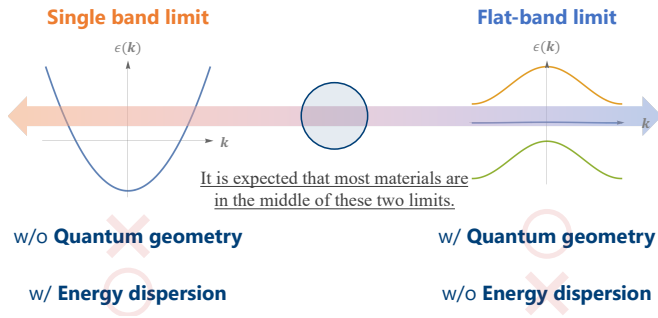


FIG. 1. Schematic illustration of the two limiting regimes of Bloch electrons. The left panel represents the single-band limit, and the right panel represents the flat-band limit. Most real materials are expected to lie between these two extremes.

## II. QUANTUM GEOMETRY IN CORRELATED ELECTRON PHASES OF FLAT-BAND SYSTEMS

The properties of Bloch electrons are described by the following eigenvalue equation:

$$H(\mathbf{k})|u_n(\mathbf{k})\rangle = \varepsilon_n(\mathbf{k})|u_n(\mathbf{k})\rangle. \quad (1)$$

Here,  $H(\mathbf{k})$  denotes the single-particle Hamiltonian in matrix representation at momentum  $\mathbf{k}$ . The energy dispersion  $\varepsilon_n(\mathbf{k})$  together with the Bloch wave function<sup>21</sup>  $|u_n(\mathbf{k})\rangle$  characterize the properties of the Bloch electrons.

Focusing on these two quantities and assuming that only a single band lies near the Fermi energy, one can identify two limiting regimes for Bloch electrons (see Fig. 1). One is the single-band limit, in which the band near the Fermi level is constructed by a single orbital that does not hybridize with other orbitals. In this limit, only the energy dispersion depends on the momentum, while the Bloch wave function is independent of  $\mathbf{k}$ . Consequently, physical phenomena are governed by the energy dispersion alone. Indeed, in a standard solid-state textbook<sup>1</sup>, a variety of topics in condensed matter physics are explained within a single-band picture by assuming, for example, a parabolic energy dispersion  $\varepsilon_n(\mathbf{k}) = k^2/2m$ .

The other is the flat-band limit, where the one band in the vicinity of the Fermi energy becomes flat, i.e.,  $\mathbf{k}$ -independent. Such a flat band originates from localized states generated by the destructive interference of Bloch wave functions due to orbital hybridization, and it appears in a variety of tight-binding models, including those on line graphs<sup>11,22</sup>. In sharp contrast to the single-band limit, only the Bloch wave function acquires a  $\mathbf{k}$ -dependence in this regime, and thus one expects physical phenomena to be characterized solely by the Bloch wave function. Although conventional wisdom has long considered many materials to effectively belong to the single-band limit, recent realizations of flat-band systems exemplified by twisted multilayer systems<sup>23,24</sup> have brought growing recognition of the importance of studying the flat-band limit.

Our interest here is to elucidate how the Bloch wave function characterizes physical phenomena in the flat-band limit. For comparison, we first discuss how the energy disper-

sion characterizes phenomena in the conventional single-band limit, with focus on superconductivity and magnetism.

### A. Single-band limit and energy dispersion

We consider the case in which the  $n$ th band constructing the Fermi surface belongs to the single-band limit. In this situation, the Bloch wave function is identically unity, i.e.,  $|u_n(\mathbf{k})\rangle = 1$ . First, we discuss superconductivity in this limit. Its hallmark phenomena are dissipationless current and the Meissner effect, which are described by the London equation,

$$\mathbf{j}_\mu = D_{\mu\nu}^s A_\nu, \quad (2)$$

where  $j_\mu$  and  $A_\nu$  denote the electric current and the vector potential along  $\mu, \nu = x, y, z$ , respectively, and  $D_{\mu\nu}^s$  is the superfluid weight. This equation indicates that superconducting responses emerge when the superfluid weight is finite.

Assuming fully gapped  $s$ -wave superconductivity for simplicity, the superfluid weight in the single-band limit is given by<sup>25-27</sup>,

$$D_{\mu\nu}^s = \frac{2}{N} \sum_{\mathbf{k}} \frac{v_n^*(\mathbf{k})}{m_n^{\mu\nu}(\mathbf{k})}, \quad (3)$$

at sufficiently low temperatures within Fermi-liquid theory. Here,  $v_n^*(\mathbf{k}) = (1 - \varepsilon_n(\mathbf{k})/E_n(\mathbf{k}))/2$  is the zero-temperature expectation value of the electron number in the superconducting state at the momentum  $\mathbf{k}$ ,  $E_n(\mathbf{k}) = \sqrt{\varepsilon_n^2(\mathbf{k}) + \Delta^2}$  is the Bogoliubov quasiparticle spectrum, and  $\Delta$  is the superconducting gap amplitude. The inverse effective-mass tensor is determined solely by the energy dispersion as  $[m_n^{\mu\nu}(\mathbf{k})]^{-1} = \partial_{k_\mu} \partial_{k_\nu} \varepsilon_n(\mathbf{k})$ . This expression shows that in the single-band limit, the superfluid weight is determined by the effective mass of Bloch electrons and the momentum distribution function.

We next turn to itinerant magnetism. Within the mean-field approximation, the magnetic order with wave vector  $\mathbf{q}$  develops when the Stoner criterion<sup>28</sup>

$$U \chi_0(\mathbf{q}) \geq 1, \quad (4)$$

is satisfied with the on-site Coulomb interaction  $U$ . In the single-band limit, the noninteracting magnetic susceptibility reads

$$\chi_0(\mathbf{q}) = \frac{1}{N} \sum_{\mathbf{k}} \frac{f(\varepsilon_n(\mathbf{k} + \mathbf{q})) - f(\varepsilon_n(\mathbf{k}))}{\varepsilon_n(\mathbf{k}) - \varepsilon_n(\mathbf{k} + \mathbf{q})}, \quad (5)$$

whose right-hand side is the Lindhard function. Here,  $f(x)$  is the Fermi-Dirac distribution function and  $N$  is the total number of unit cells. In this formula, the dominant contribution arises from momenta near the Fermi surface satisfying  $\varepsilon_n(\mathbf{k}) \sim -\varepsilon_n(\mathbf{k} + \mathbf{q})$ <sup>29</sup>. For a "nested" structure of energy dispersion, such as those realized in cuprate superconductors<sup>30</sup>, this dominant contribution leads to divergence of susceptibility. In such cases, the nesting vector  $\mathbf{q}$  that connects two momenta  $\mathbf{k}$  and  $\mathbf{k} + \mathbf{q}$  determines the stable magnetic structure.

For example, in cuprate high- $T_c$  superconductors, nesting between segments of the Fermi surface with a large density of states divergently enhances magnetic susceptibility and leads to antiferromagnetic order with  $\mathbf{q} \simeq (\pi, \pi)$ <sup>30</sup>.

Above examples illustrate that, in the single-band limit, the shape of the energy dispersion through, for example, the effective mass and nesting vector govern the physics of correlated electron phases. This is the standard textbook knowledge of condensed matter physics<sup>1,2</sup>. By analogy, we can expect that in the other extreme regime, namely the flat-band limit, it is the shape of the Bloch wave function that characterizes physical phenomena. We elaborate on this point in the next subsection.

## B. Flat-band limit and Bloch wave function

Let us consider what is meant by the ‘‘shape of the Bloch wave function’’. Because the energy dispersion is a real scalar function, its profile can be visualized directly; thus, it is evident that its curvature (the effective mass) and the constant energy contour (the nesting of the Fermi surface) characterize the ‘‘shape of the energy dispersion’’. By contrast, the Bloch wave function is a complex vector, and its shape is not as easily visualized as energy dispersion. Nevertheless, mathematics provides general frameworks to describe the ‘‘shape’’ of complex objects that are not real scalars; notable examples are topology and differential geometry. We can apply these frameworks to Bloch wave functions and have obtained a theoretical tool to study condensed matter physics. This is the concept of *quantum geometry*. In this sense, quantum geometry includes topology. The quantum geometry concerns the geometry of quantum mechanical wave functions in general. The parameters that define the geometry are not limited to the single-particle momentum, but in condensed matter physics the geometry of Bloch electrons defined in momentum space is considered in most cases.

While it has become widely appreciated that topology enables the understanding of various physical phenomena, it has recently become recognized that concepts of differential geometry applied to the Bloch wave function are useful for studying correlated electron phases<sup>13,16,17,19</sup>. A representative quantity is the Hilbert-Schmidt quantum distance:

$$D_{nm}^2(\mathbf{k}, \mathbf{q}) = 1 - |\langle u_n(\mathbf{k} + \mathbf{q}) | u_n(\mathbf{k}) \rangle|^2. \quad (6)$$

This quantity measures the distance between two Bloch states at  $\mathbf{k} + \mathbf{q}$  and  $\mathbf{k}$ : it vanishes when the two states are identical and reaches unity when they are completely different (orthogonal). For small  $\mathbf{q}$ , it admits the expansion

$$D_{nm}^2(\mathbf{k}, \mathbf{q}) \sim \sum_{\mu\nu} g_n^{\mu\nu}(\mathbf{k}) q_\mu q_\nu, \quad (7)$$

where

$$g_n^{\mu\nu}(\mathbf{k}) = \sum_{m(\neq n)} \frac{\langle \partial_{k_\mu} u_n(\mathbf{k}) | u_m(\mathbf{k}) \rangle \langle u_m(\mathbf{k}) | \partial_{k_\nu} u_n(\mathbf{k}) \rangle + \text{c.c.}}{2}. \quad (8)$$

is the quantum metric<sup>12,31</sup>. This metric encodes the infinitesimal distance between neighboring quantum states.

We should note that the Berry curvature, which characterizes the phase distance<sup>13,17</sup>, is considered to be an effective magnetic field in momentum space and is known to cause various topological phenomena<sup>5</sup>. In parallel, there is a clear physical interpretation of the quantum metric: it is the gauge-invariant part of the Wannier spread<sup>32,33</sup>, a microscopic length scale of the electronic state. Therefore, the quantum metric also naturally plays essential roles in a variety of physical phenomena. The Berry curvature and the quantum metric are related to each other through the quantum geometric tensor

$$\mathcal{G}_n^{\mu\nu}(\mathbf{k}) = \langle \partial_\mu u_n(\mathbf{k}) | \partial_\nu u_n(\mathbf{k}) \rangle - \langle \partial_\mu u_n(\mathbf{k}) | u_n(\mathbf{k}) \rangle \langle u_n(\mathbf{k}) | \partial_\nu u_n(\mathbf{k}) \rangle, \quad (9)$$

whose real and imaginary parts are the quantum metric and the Berry curvature, respectively<sup>12,31</sup>. Because the quantum geometric tensor describes the geometric properties of Bloch electrons in momentum space, it is an essential quantity in the study of quantum geometry.

Let us first turn to the superfluid weight. Assuming fully gapped  $s$ -wave superconductivity again, the superfluid weight in the flat-band limit is given by<sup>34,35</sup>,

$$D_{\mu\nu}^s = \frac{8}{N} |\Delta| \sqrt{v_n^* (1 - v_n^*)} \sum_{\mathbf{k}} g_n^{\mu\nu}(\mathbf{k}), \quad (10)$$

where we have used the fact that  $v_n^*$  is  $\mathbf{k}$ -independent in a flat-band system. Thus, in the flat-band limit, a finite quantum metric yields superconductivity. This formula indicates that in flat-band systems, where electrons in real space are localized, the supercurrent is carried via the overlap of Wannier functions, producing a finite superconducting response such as the zero resistivity and the Meissner effect. In the flat-band superconductivity of twisted-multilayer graphene<sup>36–38</sup>, the theories<sup>39–42</sup> and the experiments<sup>43–45</sup> indicate the quantum geometric origin of the superfluid weight. In certain topologically nontrivial flat-band systems, Eq. (10) is bounded from below by topological invariants including the Chern number; in such cases, superconductivity is ensured by topology<sup>34,40,46–48</sup>.

Note that Eq. (10) itself is, strictly speaking, an incomplete formula in systems with sublattice degrees of freedom<sup>49</sup>. This problem arises from the fact that the quantum metric depends on the positions of the sublattices while the superfluid weight should not in an explicit way. This issue can be resolved by taking the vertex correction into account or by replacing the quantum metric with the one minimized among all possible choices of the sublattice coordinates, namely the minimal quantum metric<sup>49</sup>. Practically, on the other hand, sublattices are often located on high-symmetry positions within a unit cell, and the quantum metric as naturally defined coincides with the minimal quantum metric. As a result, Eq. (10) is valid in many cases, and its application is sometimes found in the literature.

Magnetism likewise reflects geometric structure in the flat-band limit, where the noninteracting spin susceptibility reads,

$$\chi_0(\mathbf{q}) = \frac{1}{4TN} \sum_{\mathbf{k}} [1 - D_{nn}^2(\mathbf{k}, \mathbf{q})], \quad (11)$$

with temperature  $T$ . This formula indicates that magnetic order is determined not by Fermi-surface nesting but by the quantum distance. As the quantum distance also stabilizes the flat-band Bose-Einstein condensation<sup>50,51</sup>, its key role in stabilizing the ordered phase of flat-band systems is ubiquitous and not limited to magnetism. In particular, near  $\mathbf{q} = 0$ , we can expand<sup>52</sup>,

$$\chi_0(\mathbf{q}) \simeq \chi_0(0) - \frac{1}{4TN} \sum_{\mu\nu} \sum_{\mathbf{k}} g_n^{\mu\nu}(\mathbf{k}) q_\mu q_\nu + \dots, \quad (12)$$

where the quantum metric suppresses the susceptibility at finite  $\mathbf{q}$ . Therefore, we find that the quantum metric induces ferromagnetic correlations in flat-band systems. It was also pointed out that quantum geometry is related to the mechanism of other types of flat-band magnetism through the concept of quantum geometric nesting<sup>53–55</sup>.

The ferromagnetic instability from quantum metric is closely related to the so-called flat-band ferromagnetism<sup>11,22,56–65</sup>, where rigorous results are available<sup>11,22,56–61</sup>. The uniqueness of the ground state is ensured by quantum geometry as follows<sup>14</sup>: For the uniqueness of the ground state in flat-band ferromagnetism, an effective repulsive interaction between localized electrons in real space, which is mediated by the overlap of Wannier functions, is crucial<sup>11</sup>. Recalling again that the gauge-invariant part of the Wannier spread is the quantum metric, the quantum metric plays a central role in flat-band ferromagnetism as well. While this understanding is based on the analysis of instability from the paramagnetic phase, quantum geometry also plays a crucial role for the stability of flat-band ferromagnetism from the viewpoint of the spin stiffness<sup>62–64</sup>. In this way, the rigorous theory and the Stoner-type picture of ferromagnetism are connected through the quantum metric.

To summarize, in flat-band systems, the “shape” of the Bloch wave function, represented by the quantum metric, characterizes a wide range of physical phenomena, providing a unifying and transparent view. Indeed, qualitative behaviors of flat-band systems are dominated by quantum geometry. For example, the low-temperature scaling law of the superfluid weight arising from the quantum metric is markedly different from the conventional one anticipated from the Fermi-liquid theory<sup>42,66,67</sup>. As the temperature dependence of the superfluid weight is a standard method for probing pairing symmetry<sup>68</sup>, the scaling law of the superfluid weight is expected to be useful in determining the symmetry of flat-band superconductivity. Indeed, in twisted bilayer and trilayer graphene, which are representative flat-band systems, anomalous temperature dependences of the superfluid weight have been observed<sup>44,45</sup>, and it can be naturally explained in terms of the quantum-geometric effect<sup>42</sup>.

### III. FROM FLAT BAND TO DISPERSIVE BAND

In the previous section, we discussed the two limiting cases, namely, the single-band limit and the flat-band limit. In the latter, the “shape” of the Bloch wave function dominates the

physical phenomena, while the energy dispersion plays a central role in the former. The twisted bilayer graphene<sup>36</sup> and cuprate superconductors<sup>30</sup> may be close to the two limiting cases. However, it is expected that many materials lie in the intermediate regime between these limits. Among them are numerous systems with nontrivial quantum geometry arising from band degeneracies such as topological materials<sup>69,70</sup>, which may host unconventional phenomena unexpected from the analysis of band dispersion. In other words, dispersive-band systems can also possess nontrivial quantum geometry, driving various correlated phases. Recently, this direction has seen significant developments: various superconducting<sup>19,52,71–77</sup> and magnetic<sup>14,15,52,78–84</sup> phenomena in dispersive-band systems have been identified as being driven by quantum geometry. In particular, the quantum-geometry-driven superconducting and magnetic phenomena in flat-band systems discussed in Sec. II B carry over to electrons in certain dispersive band systems.

First, we consider the superfluid weight of multi-band systems. Assuming isotropic  $s$ -wave pairing, the superfluid weight is given by<sup>35,85</sup>,

$$\begin{aligned} D_{\mu\nu}^s &= D_{\mu\nu}^{\text{conv}} + D_{\mu\nu}^{\text{geom}}, \quad (13) \\ D_{\mu\nu}^{\text{conv}} &= \frac{2}{N} \sum_{n,\mathbf{k}} \left[ \frac{v_n^*(\mathbf{k})}{m_n^{\mu\nu}(\mathbf{k})} \tanh(E_n(\mathbf{k})/2T) \right. \\ &\quad \left. + v_n^*(\mathbf{k}) v_n^\mu(\mathbf{k}) v_n^\nu(\mathbf{k}) f'(E_n(\mathbf{k})) \right], \quad (14) \\ D_{\mu\nu}^{\text{geom}} &= 8 \frac{|\Delta|}{N} \sum_{n \neq m, \mathbf{k}} \sqrt{v_n^*(\mathbf{k})(1 - v_n^*(\mathbf{k}))} \frac{\varepsilon_m(\mathbf{k}) - \varepsilon_n(\mathbf{k})}{\varepsilon_n(\mathbf{k}) + \varepsilon_m(\mathbf{k})} \\ &\quad \times g_{nm}^{\mu\nu}(\mathbf{k}) \tanh(E_n(\mathbf{k})/2T), \quad (15) \end{aligned}$$

where  $g_{nm}^{\mu\nu}(\mathbf{k}) = \langle \partial_{k_\mu} u_n(\mathbf{k}) | u_m(\mathbf{k}) \rangle \langle u_m(\mathbf{k}) | \partial_{k_\nu} u_n(\mathbf{k}) \rangle / 2 + \text{c.c.}$  is the band-resolved quantum metric, and  $v_n^\mu(\mathbf{k}) = \partial_{k_\mu} \varepsilon_n(\mathbf{k})$  denotes the group velocity. In the single-band limit only the Fermi-liquid contribution  $D_{\mu\nu}^{\text{conv}}$  is finite, whereas in the flat-band limit, only the quantum-geometric contribution  $D_{\mu\nu}^{\text{geom}}$  remains finite. Note that, similarly to the case of Eq. (10), these formulas are also affected by the internal position of sublattices. This problem is resolved in a similar manner to the case of Eq. (10)<sup>49</sup>.

The ratio  $D_{\mu\nu}^{\text{geom}}/D_{\mu\nu}^{\text{conv}}$  is typically of the order  $|\Delta|/E_F$  with the Fermi energy  $E_F$ ; hence, in ordinary multi-band superconductors, the quantum-geometric contribution is much smaller than the Fermi-liquid contribution and has often been neglected. However, in the Bardeen-Cooper-Schrieffer (BCS)-Bose-Einstein condensation (BEC) crossover regime<sup>86</sup>,  $|\Delta|/E_F$  is in the order of unity, which implies that the quantum geometric contribution is comparable to the conventional Fermi-liquid contribution. Indeed, monolayer FeSe does not have a flat band, but is near the BCS-BEC crossover regime<sup>87–90</sup> and hosts nontrivial quantum geometry due to the band degeneracies near the Fermi level<sup>91</sup>. The quantum geometric contribution to the superfluid weight has been revealed to be comparable to the conventional term<sup>85</sup>. Moreover, it has also been shown that, in certain parameter sets, quantum geometry enhances the Berezinskii-Kosterlitz-Thouless transition temperature<sup>92,93</sup>, which corresponds to the

superconducting transition temperature of two-dimensional (2D) systems, by nearly 10K via the superfluid weight.

Next, we focus on the itinerant magnetism in multi-band systems. The noninteracting spin susceptibility of multiband systems<sup>94</sup> can be written as

$$\chi_0(\mathbf{q}) = \frac{1}{N} \sum_{\mathbf{k}} \sum_{nm} \frac{f(\varepsilon_n(\mathbf{k} + \mathbf{q})) - f(\varepsilon_m(\mathbf{k}))}{\varepsilon_m(\mathbf{k}) - \varepsilon_n(\mathbf{k} + \mathbf{q})} \times \left[ 1 - D_{nm}^2(\mathbf{k}, \mathbf{q}) \right]. \quad (16)$$

Here,  $D_{nm}^2(\mathbf{k}, \mathbf{q}) = 1 - |\langle u_n(\mathbf{k} + \mathbf{q}) | u_m(\mathbf{k}) \rangle|^2$  is the quantum distance generalized to include off-diagonal interband components. We see that the quantum distance appears in a similar manner to Eq. (11) for flat-band systems. However, in contrast to the flat-band limit, the effect of the dispersive energy band appears as in the Lindhard function, which can reflect Fermi-surface nesting. Therefore, the contributions of the energy dispersion and quantum geometry are mixed in a complicated manner.

Nevertheless, around  $\mathbf{q} = 0$  we obtain a transparent formula<sup>52</sup> as,

$$\chi_0(\mathbf{q}) = \chi_0(0) + \sum_{\mu\nu} (\chi_{\text{geom}}^{\mu\nu} + \chi_{\text{mass}}^{\mu\nu}) q_\mu q_\nu + \dots, \quad (17)$$

$$\chi_{\text{geom}}^{\mu\nu} = \sum_n \int \frac{d\mathbf{k}}{(2\pi)^2} [2f'(\varepsilon_n(\mathbf{k})) g_n^{\mu\nu}(\mathbf{k}) + 4f(\varepsilon_n(\mathbf{k})) X_n^{\mu\nu}(\mathbf{k})], \quad (18)$$

$$\chi_{\text{mass}}^{\mu\nu} = - \sum_n \int \frac{d\mathbf{k}}{(2\pi)^2} \frac{f^{(2)}(\varepsilon_n(\mathbf{k}))}{6} [m_n^{\mu\nu}(\mathbf{k})]^{-1}, \quad (19)$$

where the quadratic coefficient in  $\mathbf{q}$  is decomposed as  $\chi_c^{\mu\nu} = \chi_{\text{geom}}^{\mu\nu} + \chi_{\text{mass}}^{\mu\nu}$ . Here,  $\chi_{\text{geom}}^{\mu\nu}$  is the quantum geometric term originating from the quantum distance, which contains the quantum metric  $g_n^{\mu\nu}(\mathbf{k})$  in addition to another geometric quantity called positional shift (or Berry connection polarizability),  $X_n^{\mu\nu}(\mathbf{k}) = \sum_{m(\neq n)} g_{nm}^{\mu\nu}(\mathbf{k}) / (\varepsilon_m(\mathbf{k}) - \varepsilon_n(\mathbf{k}))$ <sup>95</sup>. The second term  $\chi_{\text{mass}}^{\mu\nu}$  is the effective-mass contribution originating from the Lindhard function and is determined by the energy dispersion.

The quadratic coefficient  $\chi_c^{\mu\nu} = \chi_{\text{geom}}^{\mu\nu} + \chi_{\text{mass}}^{\mu\nu}$  represents the curvature of susceptibility and plays a key role for examining ferromagnetism: if  $\chi_c^{\mu\nu}$  is positive semidefinite,  $\chi_0(\mathbf{q})$  does not peak at  $\mathbf{q} = 0$  and ferromagnetism is prohibited. In contrast, a negative definite  $\chi_c^{\mu\nu}$  implies that  $\chi_0(0)$  is a local maximum, indicating the presence of ferromagnetic correlations. Thus,  $\chi_c$  serves as an indicator of ferromagnetism. Analysis of this quantity provides a transparent view of the role of quantum geometry. In the quantum geometric term  $\chi_{\text{geom}}^{\mu\nu}$ , the contribution involving the positional shift is positive, whereas the contribution involving the quantum metric is negative and thus promotes ferromagnetic correlations. This is consistent with the discussion in Sec. II B, where a close relation between the quantum metric and flat-band ferromagnetism is discussed. In other words, the concept of flat-band ferromagnetism can be generalized to dispersive band systems by utilizing the quantum metric. Even when the effective-mass term disfavors ferromagnetism, the quantum geometric

term can overcome it, resulting in *quantum geometric ferromagnetism*. Stimulated by this discovery, the competition between quantum geometric and energy-dispersion effects on the magnetism has attracted much attention<sup>14,15,78,79,83,84</sup>, and an approach based on the effective spin model has also been proposed recently<sup>80</sup>.

A typical platform for quantum geometric ferromagnetism is a 2D  $t_{2g}$ -orbital model with symmetry-protected band degeneracies<sup>14</sup>. It is shown that<sup>14</sup>, in most parameters where band touching lies on Fermi surfaces, the 2D  $t_{2g}$ -orbital model exhibits quantum geometric ferromagnetism. The band-touching point in this model is accompanied by a saddle-point structure with a divergent density of states (DOS), which is the so-called singular saddle point. The divergent quantum metric induces the ferromagnetic correlation despite the effective mass being disadvantageous for it, and the divergent DOS ensures the Stoner criteria. Therefore, it is expected that the singular saddle point is a promising platform for quantum geometric ferromagnetism, which is not restricted to a specific model.

Moreover, in the same 2D  $t_{2g}$ -orbital model, a flat band emerges at a certain parameter set. In this case, we can rigorously prove the ferromagnetic ground state by using the theory of flat-band ferromagnetism<sup>14</sup>. Hence, quantum geometric ferromagnetism is continuously connected to flat-band ferromagnetism. It follows that the essence of flat-band ferromagnetism is taken over to dispersive band systems through the divergent quantum metric due to the band touching.

#### IV. SUMMARY AND OUTLOOK

In summary, the properties of Bloch electrons are described by the energy spectrum and the Bloch wave function, whose shape in momentum space, that is, energy dispersion and quantum geometry, respectively, characterize various phenomena in condensed matter physics. In particular, Bloch electrons possess two characteristic quantum geometric structures: one is the phase distance described by the Berry curvature, and the other is the amplitude distance related to the quantum metric. While the Berry curvature plays essential roles in various topological phenomena as an effective magnetic field, the quantum metric serves as the spread of the Wannier function, enriching a variety of correlated electron phases.

Flat-band systems without energy dispersion offer a paradigmatic platform for correlated electron phases dominated by quantum geometry and central topics for studying quantum geometry. However, we have shown that the quantum geometric effect can be taken over to the dispersive-band systems without a flat band; various types of superconductivity and magnetism can be driven by quantum geometry. While we focus on the superfluid weight and ferromagnetism, quantum geometry also plays a significant role in other superconducting and magnetic phenomena. For example, quantum geometry induces finite momentum superconductivity, including Fulde–Ferrell–Larkin–Ovchinnikov superconductivity<sup>73</sup> and anapole superconductivity<sup>74</sup>, which have flat-band counter-

parts<sup>82,96–98</sup>. As for magnetism, recent progress has shown that the quantum-geometry-driven magnetism is not limited to ferromagnetism: antiferromagnetism<sup>15</sup>, altermagnetism<sup>78</sup>, and odd-parity magnetism<sup>79</sup> can be driven by quantum geometry. Moreover, the quantum geometric origins of magnetism in the real materials, LaFeAsO and Pb<sub>9</sub>Cu(PO<sub>4</sub>)<sub>6</sub>O, are revealed by the first-principles calculations<sup>84</sup>.

Beyond the phenomena covered in this perspective, quantum geometry manifests itself in many other contexts. In addition to well-known transport responses<sup>8,9</sup>, it plays roles in correlated electron physics, such as the electron-phonon coupling phenomena<sup>99–104</sup>, fractional Chern insulators<sup>20</sup>, Bose-Einstein condensation<sup>50,51</sup>, and screened Coulomb interaction<sup>105,106</sup>. As we have seen, even in problems traditionally thought to be governed primarily by the energy dispersion, consideration of flat-band systems shows that the phenomena are necessarily controlled by quantum geometry, and these effects carry over to dispersive-band systems as well. We hope that this article will help catalyze further research on quantum geometry, leading to the recognition of its importance across diverse phenomena and to the discovery of yet unrecognized physics.

## ACKNOWLEDGMENTS

We are grateful to T. Yamashita, J. Ishizuka, S. Kanasugi, M. Chazono, H. Nakai, C.G. Oh, J.W. Rhim, M. Ichikawa, M. Fujimoto, H. Hirobe, H. Katsura, R. Arita, and H. Watanabe for fruitful comments and discussions. This work was supported by JSPS KAKENHI (Grant No. JP25K23367, No. JP18H01178, No. JP18H05227, No. JP20H05159, No. JP21K18145, No. JP22H01181, No. JP22H04933, No. JP21K13880, No. JP23K17353, No. JP24H01662, No. JP23KK0248, No. JP24H00007, No. JP24K21530, No. JP25H01249).

## DATA AVAILABILITY STATEMENT

The data that support the findings of this study are available from the corresponding author upon reasonable request.

- <sup>1</sup>G. D. Mahan, *Many-particle physics*, Physics of Solids and Liquids (Springer, Berlin, 2010).
- <sup>2</sup>A. Altland and B. D. Simons, *Condensed Matter Field Theory*, 2nd ed. (Cambridge University Press, 2010).
- <sup>3</sup>M. Z. Hasan and C. L. Kane, “Colloquium: Topological insulators,” *Rev. Mod. Phys.* **82**, 3045–3067 (2010).
- <sup>4</sup>X.-L. Qi and S.-C. Zhang, “Topological insulators and superconductors,” *Rev. Mod. Phys.* **83**, 1057–1110 (2011).
- <sup>5</sup>N. Nagaosa, J. Sinova, S. Onoda, A. H. MacDonald, and N. P. Ong, “Anomalous Hall effect,” *Rev. Mod. Phys.* **82**, 1539–1592 (2010).
- <sup>6</sup>I. Sodemann and L. Fu, “Quantum Nonlinear Hall Effect Induced by Berry Curvature Dipole in Time-Reversal Invariant Materials,” *Phys. Rev. Lett.* **115**, 216806 (2015).
- <sup>7</sup>N. Nagaosa and T. Morimoto, “Concept of Quantum Geometry in Optoelectronic processes in Solids: Application to Solar Cells,” *Adv. Mater.* **29** (2017).
- <sup>8</sup>T. Liu, X.-B. Qiang, H.-Z. Lu, and X. C. Xie, “Quantum geometry in condensed matter,” *Natl. Sci. Rev.* **12**, nwae334 (2025).

- <sup>9</sup>A. Gao, N. Nagaosa, N. Ni, and S.-Y. Xu, “Quantum geometry phenomena in condensed matter systems,” (2025), arXiv:2508.00469 [cond-mat.str-el].
- <sup>10</sup>K. Kuroki, S. Onari, R. Arita, H. Usui, Y. Tanaka, and others, “Unconventional Pairing Originating from the Disconnected Fermi Surfaces of Superconducting LaFeAsO<sub>1-x</sub>F<sub>x</sub>,” *Phys. Rev. Lett.* (2008).
- <sup>11</sup>H. Tasaki, “Physics and mathematics of quantum many-body systems,” (Springer, Berlin, 2020).
- <sup>12</sup>R. Resta, “The insulating state of matter: a geometrical theory,” *Eur. Phys. J. B* **79**, 121–137 (2011).
- <sup>13</sup>P. Törmä, “Essay: Where Can Quantum Geometry Lead Us?” *Phys. Rev. Lett.* **131**, 240001 (2023).
- <sup>14</sup>T. Kitamura, H. Nakai, A. Daido, and Y. Yanase, “Quantum geometric ferromagnetism by singular saddle point,” (2025), arXiv:2505.01089 [cond-mat.str-el].
- <sup>15</sup>C.-g. Oh, T. Kitamura, A. Daido, J.-W. Rhim, and Y. Yanase, “Magnetic phase transitions driven by quantum geometry,” (2025), arXiv:2509.13618 [cond-mat.str-el].
- <sup>16</sup>E. Rossi, “Quantum metric and correlated states in two-dimensional systems,” *Curr. Opin. Solid State Mater. Sci.* **25**, 100952 (2021).
- <sup>17</sup>P. Törmä, S. Peotta, and B. A. Bernevig, “Superconductivity, superfluidity and quantum geometry in twisted multilayer systems,” *Nature Reviews Physics* **4**, 528 (2022).
- <sup>18</sup>S. Peotta, K.-E. Huhtinen, and P. Törmä, “Quantum geometry in superfluidity and superconductivity,” (2023), arXiv:2308.08248 [cond-mat.quant-gas].
- <sup>19</sup>J. Yu, B. A. Bernevig, R. Queiroz, E. Rossi, P. Törmä, and B.-J. Yang, “Quantum geometry in quantum materials,” *Npj Quantum Mater.* **10**, 1–19 (2025).
- <sup>20</sup>Z. Liu and E. J. Bergholtz, “Recent developments in fractional Chern insulators,” in *Encyclopedia of Condensed Matter Physics* (Elsevier, 2024) pp. 515–538.
- <sup>21</sup>Strictly speaking,  $|u_n(\mathbf{k})\rangle$  is the periodic part of the Bloch wave function  $e^{i\mathbf{k}\cdot\mathbf{r}}|u_n(\mathbf{k})\rangle$ . In what follows, however, we simply refer to  $|u_n(\mathbf{k})\rangle$  as the Bloch wave function.
- <sup>22</sup>A. Mielke, “Ferromagnetic ground states for the Hubbard model on line graphs,” *J. Phys. A Math. Gen.* **24**, L73–L77 (1991).
- <sup>23</sup>E. Y. Andrei, D. K. Efetov, P. Jarillo-Herrero, A. H. MacDonald, K. F. Mak, T. Senthil, E. Tutuc, A. Yazdani, and A. F. Young, “The marvels of moiré materials,” *Nature Reviews Materials* **6**, 201–206 (2021).
- <sup>24</sup>K. P. Nuckolls and A. Yazdani, “A microscopic perspective on moiré materials,” *Nat. Rev. Mater.* **9**, 460–480 (2024).
- <sup>25</sup>D. J. Scalapino, S. R. White, and S. C. Zhang, “Superfluid density and the Drude weight of the Hubbard model,” *Phys. Rev. Lett.* **68**, 2830–2833 (1992).
- <sup>26</sup>D. J. Scalapino, S. R. White, and S. Zhang, “Insulator, metal, or superconductor: The criteria,” *Phys. Rev. B Condens. Matter* **47**, 7995–8007 (1993).
- <sup>27</sup>T. Jujo, “Fermi liquid theory on transport phenomena in the superconducting state,” *J. Phys. Soc. Jpn.* **70**, 1349–1363 (2001).
- <sup>28</sup>J. Hubbard, “Electron correlations in narrow energy bands,” *Proc. R. Soc. Lond.* **276**, 238–257 (1963).
- <sup>29</sup>As in iron-based superconductors<sup>107</sup>, nesting between electron and hole Fermi pockets can induce a  $\log T$  divergence in susceptibility, and the corresponding nesting vectors connect momenta at which the velocities carry opposite signs.
- <sup>30</sup>Y. Yanase, T. Jujo, T. Nomura, H. Ikeda, T. Hotta, and K. Yamada, “Theory of superconductivity in strongly correlated electron systems,” *Phys. Rep.* **387**, 1 (2003).
- <sup>31</sup>J. P. Provost and G. Vallee, “Riemannian structure on manifolds of quantum states,” *Commun. Math. Phys.* **76**, 289–301 (1980).
- <sup>32</sup>N. Marzari and D. Vanderbilt, “Maximally localized generalized Wannier functions for composite energy bands,” *Phys. Rev. B Condens. Matter* **56**, 12847–12865 (1997).
- <sup>33</sup>D. Vanderbilt, “Berry phases in electronic structure theory: Electric polarization, orbital magnetization and topological insulators,” (Cambridge University Press, 2018).
- <sup>34</sup>S. Peotta and P. Törmä, “Superfluidity in topologically nontrivial flat bands,” *Nat. Commun.* **6**, 8944 (2015).

- <sup>35</sup>L. Liang, T. I. Vanhala, S. Peotta, T. Siro, A. Harju, and P. Törmä, “Band geometry, Berry curvature, and superfluid weight,” *Phys. Rev. B Condens. Matter* **95**, 024515 (2017).
- <sup>36</sup>Y. Cao, V. Fatemi, S. Fang, K. Watanabe, T. Taniguchi, E. Kaxiras, and P. Jarillo-Herrero, “Unconventional superconductivity in magic-angle graphene superlattices,” *Nature* **556**, 43–50 (2018).
- <sup>37</sup>Z. Hao, A. M. Zimmerman, P. Ledwith, E. Khalaf, D. H. Najafabadi, K. Watanabe, T. Taniguchi, A. Vishwanath, and P. Kim, “Electric field-tunable superconductivity in alternating-twist magic-angle trilayer graphene,” *Science* **371**, 1133–1138 (2021).
- <sup>38</sup>J. M. Park, Y. Cao, K. Watanabe, T. Taniguchi, and P. Jarillo-Herrero, “Tunable strongly coupled superconductivity in magic-angle twisted trilayer graphene,” *Nature* **590**, 249–255 (2021).
- <sup>39</sup>X. Hu, T. Hyart, D. I. Pikulin, and E. Rossi, “Geometric and Conventional Contribution to the Superfluid Weight in Twisted Bilayer Graphene,” *Phys. Rev. Lett.* **123**, 237002 (2019).
- <sup>40</sup>F. Xie, Z. Song, B. Lian, and B. A. Bernevig, “Topology-Bounded Superfluid Weight in Twisted Bilayer Graphene,” *Phys. Rev. Lett.* **124**, 167002 (2020).
- <sup>41</sup>A. Julku, T. J. Peltonen, L. Liang, T. T. Heikkilä, and P. Törmä, “Superfluid weight and Berezinskii-Kosterlitz-Thouless transition temperature of twisted bilayer graphene,” *Phys. Rev. B: Condens. Matter Mater. Phys.* (2020).
- <sup>42</sup>Y. Hirobe, T. Kitamura, and Y. Yanase, “Anomalous Temperature Dependence of Quantum-Geometric Superfluid Weight,” (2025), arXiv:2505.13065 [cond-mat.supr-con].
- <sup>43</sup>H. Tian, X. Gao, Y. Zhang, S. Che, T. Xu, P. Cheung, K. Watanabe, T. Taniguchi, M. Randeria, F. Zhang, C. N. Lau, and M. W. Bockrath, “Evidence for Dirac flat band superconductivity enabled by quantum geometry,” *Nature* **614**, 440–444 (2023).
- <sup>44</sup>M. Tanaka, J. I.-j. Wang, T. H. Dinh, D. Rodan-Legrain, S. Zaman, M. Hays, A. Almanakly, B. Kannan, D. K. Kim, B. M. Niedzielski, K. Sereniak, M. E. Schwartz, K. Watanabe, T. Taniguchi, T. P. Orlando, S. Gustavsson, J. A. Grover, P. Jarillo-Herrero, and W. D. Oliver, “Superfluid stiffness of magic-angle twisted bilayer graphene,” *Nature* **638**, 99–105 (2025).
- <sup>45</sup>A. Banerjee, Z. Hao, M. Kreidel, P. Ledwith, I. Phinney, J. M. Park, A. Zimmerman, M. E. Wesson, K. Watanabe, T. Taniguchi, R. M. Westervelt, A. Yacoby, P. Jarillo-Herrero, P. A. Volkov, A. Vishwanath, K. C. Fong, and P. Kim, “Superfluid stiffness of twisted trilayer graphene superconductors,” *Nature* **638**, 93–98 (2025).
- <sup>46</sup>J. Herzog-Arbeitman, V. Peri, F. Schindler, S. D. Huber, and B. A. Bernevig, “Superfluid Weight Bounds from Symmetry and Quantum Geometry in Flat Bands,” *Phys. Rev. Lett.* **128**, 087002 (2022).
- <sup>47</sup>J. Yu, M. Xie, F. Wu, and S. Das Sarma, “Euler-obstructed nematic nodal superconductivity in twisted bilayer graphene,” *Phys. Rev. B Condens. Matter* **107**, L201106 (2023).
- <sup>48</sup>T. Prijon, S. D. Huber, and K.-E. Huhtinen, “Superfluid stiffness of superconductors with delicate topology,” (2025), arXiv:2507.16909 [cond-mat.supr-con].
- <sup>49</sup>K.-E. Huhtinen, J. Herzog-Arbeitman, A. Chew, B. A. Bernevig, and P. Törmä, “Revisiting flat band superconductivity: Dependence on minimal quantum metric and band touchings,” *Phys. Rev. B* **106**, 014518 (2022).
- <sup>50</sup>A. Julku, G. M. Bruun, and P. Törmä, “Quantum Geometry and Flat Band Bose-Einstein Condensation,” *Phys. Rev. Lett.* **127**, 170404 (2021).
- <sup>51</sup>A. Julku, G. M. Bruun, and P. Törmä, “Excitations of a Bose-Einstein condensate and the quantum geometry of a flat band,” *Phys. Rev. B* **104**, 144507 (2021).
- <sup>52</sup>T. Kitamura, A. Daido, and Y. Yanase, “Spin-Triplet Superconductivity from Quantum-Geometry-Induced Ferromagnetic Fluctuation,” *Phys. Rev. Lett.* **132**, 036001 (2024).
- <sup>53</sup>Z. Han, J. Herzog-Arbeitman, B. A. Bernevig, and S. A. Kivelson, “Quantum Geometric Nesting” and Solvable Model Flat-Band Systems,” *Phys. Rev. X* **14**, 041004 (2024).
- <sup>54</sup>J.-X. Zhang, W. O. Wang, L. Balents, and L. Savary, “Identifying instabilities with quantum geometry in flat band systems,” (2025), arXiv:2504.03882 [cond-mat.str-el].
- <sup>55</sup>Z.-T. Sun, R.-P. Yu, S. A. Chen, J.-X. Hu, and K. T. Law, “Flat-band Fulde-Ferrell-Larkin-Ovchinnikov state from quantum geometric discrepancy,” *Quantum Front.* **4**, 20 (2025).
- <sup>56</sup>A. Mielke, “Exact ground states for the Hubbard model on the Kagome lattice,” *J. Phys. A Math. Gen.* **25**, 4335–4345 (1992).
- <sup>57</sup>H. Tasaki, “Ferromagnetism in the Hubbard models with degenerate single-electron ground states,” *Phys. Rev. Lett.* **69**, 1608–1611 (1992).
- <sup>58</sup>A. Mielke and H. Tasaki, “Ferromagnetism in the Hubbard model,” *Commun. Math. Phys.* **158**, 341–371 (1993).
- <sup>59</sup>H. Tasaki, “Ferromagnetism in Hubbard models,” *Phys. Rev. Lett.* **75**, 4678–4681 (1995).
- <sup>60</sup>A. Mielke, “Stability of ferromagnetism in Hubbard models with degenerate single-particle ground states,” *J. Phys. A Math. Gen.* **32**, 8411–8418 (1999).
- <sup>61</sup>H. Katsura, I. Maruyama, A. Tanaka, and H. Tasaki, “Ferromagnetism in the Hubbard model with topological/non-topological flat bands,” *EPL* **91**, 57007 (2010).
- <sup>62</sup>F. Wu and S. Das Sarma, “Quantum geometry and stability of moiré flat-band ferromagnetism,” *Phys. Rev. B Condens. Matter* **102**, 165118 (2020).
- <sup>63</sup>J. Kang, T. Oh, J. Lee, and B.-J. Yang, “Quantum geometric bound for saturated ferromagnetism,” (2024), arXiv:2402.07171 [cond-mat.str-el].
- <sup>64</sup>J. Herzog-Arbeitman, A. Chew, K.-E. Huhtinen, P. Törmä, and B. A. Bernevig, “Many-body superconductivity in topological flat bands,” (2022), arXiv:2209.00007 [cond-mat.str-el].
- <sup>65</sup>F. Pichler, C. Kuhlenskamp, and M. Knap, “False vacuum decay in flat-band ferromagnets: Role of quantum geometry and chiral edge states,” (2025), arXiv:2512.13786 [cond-mat.str-el].
- <sup>66</sup>M. Buthenhoff and Y. Nishida, “Low-temperature scaling laws in unconventional flat-band superconductors,” (2025), arXiv:2510.23159 [cond-mat.supr-con].
- <sup>67</sup>R. P. S. Penttilä, K.-E. Huhtinen, and P. Törmä, “Flat-band ratio and quantum metric in the superconductivity of modified Lieb lattices,” *Commun. Phys.* **8**, 50 (2025).
- <sup>68</sup>W. N. Hardy, D. A. Bonn, D. C. Morgan, R. Liang, and K. Zhang, “Precision measurements of the temperature dependence of lambda in  $\text{YBa}_2\text{Cu}_3\text{O}_{6.95}$ : Strong evidence for nodes in the gap function,” *Phys. Rev. Lett.* **70**, 3999–4002 (1993).
- <sup>69</sup>M. G. Vergniory, L. Elcoro, C. Felser, N. Regnault, B. A. Bernevig, and Z. Wang, “A complete catalogue of high-quality topological materials,” *Nature* **566**, 480–485 (2019).
- <sup>70</sup>T. Zhang, Y. Jiang, Z. Song, H. Huang, Y. He, Z. Fang, H. Weng, and C. Fang, “Catalogue of topological electronic materials,” *Nature* **566**, 475–479 (2019).
- <sup>71</sup>J. Ahn and N. Nagaosa, “Superconductivity-induced spectral weight transfer due to quantum geometry,” *Phys. Rev. B Condens. Matter* **104**, L100501 (2021).
- <sup>72</sup>W. Chen and W. Huang, “Quantum-geometry-induced intrinsic optical anomaly in multiorbital superconductors,” *Phys. Rev. Research* **3**, L042018 (2021).
- <sup>73</sup>T. Kitamura, A. Daido, and Y. Yanase, “Quantum geometric effect on Fulde-Ferrell-Larkin-Ovchinnikov superconductivity,” *Phys. Rev. B Condens. Matter* **106**, 184507 (2022).
- <sup>74</sup>T. Kitamura, S. Kanasugi, M. Chazono, and Y. Yanase, “Quantum geometry induced anapole superconductivity,” *Phys. Rev. B Condens. Matter* **107**, 214513 (2023).
- <sup>75</sup>A. Daido, T. Kitamura, and Y. Yanase, “Quantum geometry encoded to pair potentials,” *Phys. Rev. B* **110**, 094505 (2024).
- <sup>76</sup>J.-L. Zhang, W. Chen, H.-T. Liu, Y. Li, Z. Wang, and W. Huang, “Quantum-Geometry-Induced Anomalous Hall Effect in Nonunitary Superconductors and Application to  $\text{Sr}_2\text{RuO}_4$ ,” *Phys. Rev. Lett.* **132**, 136001 (2024).
- <sup>77</sup>F. Simon, “Normal-state quantum geometry, nonlocality, and superconductivity,” *Phys. Rev. B* **112**, 104504 (2025).
- <sup>78</sup>N. Heinsdorf, “Altermagnetic instabilities from quantum geometry,” *Phys. Rev. B* **111**, 174407 (2025).
- <sup>79</sup>K. Kudo and Y. Yanase, “Odd-parity magnetism by quantum geometry,” (2025), arXiv:2505.20907 [cond-mat.str-el].
- <sup>80</sup>H. Hu, O. Vafek, K. Haule, and B. A. Bernevig, “Ferromagnetism vs. Antiferromagnetism in Narrow-Band Systems: Competition Between Quantum Geometry and Band Dispersion,” (2025), arXiv:2509.03575 [cond-mat.str-el].

- <sup>81</sup>A. de Jesús Espinosa-Champo and G. G. Naumis, “Magnetic phase transitions protected by topological quantum geometry transitions: effects of electron-electron interactions in the Creutz ladder system,” (2025), arXiv:2509.26320 [cond-mat.str-el].
- <sup>82</sup>H.-X. Wang and W. Huang, “Density matrix renormalization group study of the quantum-geometry-facilitated pair density wave order,” *Sci. China Phys. Mech. Astron.* **68**, 1–7 (2025).
- <sup>83</sup>K. Nogaki and Y. Yanase, “Quantum geometric magnetic monopole and two-phase superconductivity in  $\text{CeRh}_2\text{As}_2$ ,” (2025), arXiv:2510.24289 [cond-mat.supr-con].
- <sup>84</sup>M. Shimizu, C. guen Oh, and Y. Yanase, “Magnetic fluctuations driven by quantum geometry,” (2026), arXiv:2602.14511 [cond-mat.str-el].
- <sup>85</sup>T. Kitamura, T. Yamashita, J. Ishizuka, A. Daido, and Y. Yanase, “Superconductivity in monolayer FeSe enhanced by quantum geometry,” *Phys. Rev. Research* **4**, 023232 (2022).
- <sup>86</sup>P. Nozières and S. Schmitt-Rink, “Bose condensation in an attractive fermion gas: From weak to strong coupling superconductivity,” *Journal of Low Temperature Physics* **59**, 195–211 (1985).
- <sup>87</sup>S. Kasahara, T. Watashige, T. Hanaguri, Y. Kohsaka, T. Yamashita, Y. Shimoyama, Y. Mizukami, R. Endo, H. Ikeda, K. Aoyama, T. Terashima, S. Uji, T. Wolf, H. von Löhneysen, T. Shibauchi, and Y. Matsuda, “Field-induced superconducting phase of FeSe in the BCS-BEC cross-over,” *Proceedings of the National Academy of Sciences* **111**, 16309–16313 (2014), <https://www.pnas.org/content/111/46/16309.full.pdf>.
- <sup>88</sup>S. Kasahara, T. Yamashita, A. Shi, R. Kobayashi, Y. Shimoyama, T. Watashige, K. Ishida, T. Terashima, T. Wolf, F. Hardy, C. Meingast, H. v. Löhneysen, A. Levchenko, and Y. Shibauchi, T.and Matsuda, “Giant superconducting fluctuations in the compensated semimetal FeSe at the BCS–BEC crossover,” *Nature Communications* **7**, 12843 (2016).
- <sup>89</sup>T. Hanaguri, S. Kasahara, J. Böker, I. Eremin, T. Shibauchi, and Y. Matsuda, “Quantum Vortex Core and Missing Pseudogap in the Multiband BCS-BEC Crossover Superconductor FeSe,” *Phys. Rev. Lett.* **122**, 077001 (2019).
- <sup>90</sup>S. Kasahara, Y. Sato, S. Licciardello, M. Čulo, S. Arsenijević, T. Ottenbros, T. Tominaga, J. Böker, I. Eremin, T. Shibauchi, J. Wosnitza, N. E. Hussey, and Y. Matsuda, “Evidence for an Fulde-Ferrell-Larkin-Ovchinnikov State with Segmented Vortices in the BCS-BEC-Crossover Superconductor FeSe,” *Phys. Rev. Lett.* **124**, 107001 (2020).
- <sup>91</sup>T. Kitamura, J. Ishizuka, A. Daido, and Y. Yanase, “Thermodynamic electric quadrupole moments of nematic phases from first-principles calculations,” *Phys. Rev. B Condens. Matter* **103**, 245114 (2021).
- <sup>92</sup>J. M. Kosterlitz and D. J. Thouless, “Ordering, metastability and phase transitions in two-dimensional systems,” *J. Phys. C: Solid State Phys.* **6**, 1181 (1973).
- <sup>93</sup>V. L. Berezinskii, “Destruction of long-range order in one-dimensional and two-dimensional systems having a continuous symmetry group I. classical systems,” *Sov. Phys. JETP* **32**, 493–500 (1971).
- <sup>94</sup>Here we assume the absence of the spin-orbit coupling for simplicity.
- <sup>95</sup>Y. Gao, S. A. Yang, and Q. Niu, “Field Induced Positional Shift of Bloch Electrons and Its Dynamical Implications,” *Phys. Rev. Lett.* **112**, 166601 (2014).
- <sup>96</sup>G. Jiang and Y. Barlas, “Pair Density Waves from Local Band Geometry,” *Phys. Rev. Lett.* **131**, 016002 (2023).
- <sup>97</sup>W. Chen and W. Huang, “Pair density wave facilitated by Bloch quantum geometry in nearly flat band multiorbital superconductors,” *Sci. China Ser. G: Phys. Mech. Astron.* **66**, 287212 (2023).
- <sup>98</sup>A. Dunbrack, P. Virtanen, and T. T. Heikkilä, “Quantum geometry of time-reversal symmetry breaking in flat-band superconductivity,” (2025), arXiv:2503.14721 [cond-mat.supr-con].
- <sup>99</sup>L.-H. Hu, J. Yu, I. Garate, and C.-X. Liu, “Phonon Helicity Induced by Electronic Berry Curvature in Dirac Materials,” *Phys. Rev. Lett.* **127**, 125901 (2021).
- <sup>100</sup>J. Yu, C. J. Ciccarino, R. Bianco, I. Errea, P. Narang, and B. A. Bernevig, “Non-trivial quantum geometry and the strength of electron–phonon coupling,” *Nature Physics* **20**, 1262–1268 (2024).
- <sup>101</sup>J. Hu, W. Li, Z. Guo, H. Wang, and K. Chang, “Quantum Geometry in Phonon-Mediated Optical Responses,” *Phys. Rev. Lett.* **135**, 256404 (2025).
- <sup>102</sup>J. Hu, Z. Zhu, Y. Yuan, H. Wang, and K. Chang, “Quantum Geometric Origin of Strain-Induced Ferroelectric Phase Transitions,” *Phys. Rev. Lett.* **135**, 256405 (2025).
- <sup>103</sup>G. Pellitteri, Z. Dai, H. Hu, Y. Jiang, G. Menichetti, A. Tomadin, B. A. Bernevig, and M. Polini, “Phonon spectra, quantum geometry, and the Goldstone theorem,” (2025), arXiv:2502.04221 [cond-mat.mes-hall].
- <sup>104</sup>D. Li, G. Yang, T. Qin, J. Zhou, and Y. Yao, “Phonon dichroisms revealing unusual electronic quantum geometry,” (2025), arXiv:2511.16141 [cond-mat.mes-hall].
- <sup>105</sup>G. Shavit and J. Alicea, “Quantum Geometric Kohn-Luttinger Superconductivity,” *Phys. Rev. Lett.* **134**, 176001 (2025).
- <sup>106</sup>G. Shavit, “Nematic Enhancement of Superconductivity in Multilayer Graphene via Quantum Geometry,” (2025), arXiv:2509.13407 [cond-mat.supr-con].